INITIAL STIFFNESS OF REVERSE CHANNEL CONNECTIONS

Tim Heistermann[a], Efthymios Koltsakis[a], Milan Veljkovic[a], Fernanda Lopes[a], Aldina Santiago[b], Luís Simões da Silva[b]

[a]Luleå University of Technology, Division of Structural and Construction Engineering, Sweden
timhei@ltu.se, eftkol@ltu.se, milan@ltu.se
[b] University of Coimbra, ISISE, Civil Engineering Department, Portugal
fernanda@dec.uc.pt, aldina@dec.uc.pt, luisss@dec.uc.pt

INTRODUCTION

In fire situations constraining the thermal expansion of beams, results to premature and unpredictable failures. The connection studied in the present paper precisely remedies this particular issue. As present design codes [1,2] provide relatively little information on the behaviour of connections at elevated temperature, this study attempts to quantify the stiffness that the reverse channel (RC) connections (see *Fig.1*) provides against the free thermal dilation of a beam. Observations made in real fire situations, such as for the collapse of the World Trade Center [3,4] and during a full-scale fire test at Cardington [5] have clearly shown the importance of joints with respect to the robustness. During a fire the structure undergoes essential changes due to degradation of material properties and internal forces, which may change rapidly due to restrained thermal deformations. This connection is particularly applicable for connecting beams to either circular or rectangular (concrete filled) hollow-section columns. The flanges of the channel section are welded to the column face and the channel web is bolted to a conventional endplate on the beam side [6].

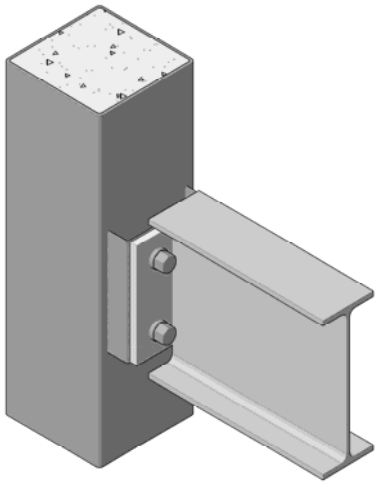

Fig. 1. Reverse channel joint – partial-depth endplate configuration

However, there is a lack of analytical design recommendations for this kind of connection both at ambient and elevated temperature. In the context of the component method [1], a characterisation of the behaviour of the new component – the reverse channel section – in tension and in compression is necessary. Therefore, this paper provides analytical solutions to prescribe the initial stiffness of different reverse channel – partial-depth endplate connections in compression and tension at constant temperatures. An experimental programme was performed at the University of Coimbra to investigate the behaviour of channel sections loaded transversely through their web at ambient and elevated temperatures. The experimental programme consisted of 13 tensile and 8 compressive tests in order to better understand the overall behaviour of the component; to establish relationships between force, displacement and temperature; and to study the influence of one of the most relevant parameters, its slenderness [7]. In order to verify the experimental results, 3D Finite Element simulations of all tests have been carried out with the commercial software ABAQUS [8]. A wide range of 2D plane-stress FE simulations is carried out to verify the analytical solutions.

1 NUMERICAL WORK

1.1 Introduction

The stiffness assessment of the reverse channel sections in compression and tension is verified by means of 2D and 3D Finite Element simulations. 2D simulations are carried out in order to verify the analytical solutions which are frame theory based. They provide less time consuming (compared to full 3D simulations) calculations and therefore offer the capability of enlarged parametric studies. Establishing sufficient coincidence between the frame theory (analytic) approach and 2D plane-stress FE models was a first step. Having done this, one should use full 3D simulations to establish the way the system behaves as it becomes longer.

1.2 Parametric studies

Different parametric studies are carried out in order to investigate their parameter's effect on the initial stiffness. They are designed to understand the problem and to support the derivation of analytical solutions by means of identifying contact zones between the reverse channel and endplate.

The following parameters have been studied:

- *Leg length H*
- *Bolt spacing (CC′)*
- *Endplate thickness*
- *Reverse channel thickness*
- *Endplate tail length (BC)*
- *Temperature*

Perfect 2D-3D coincidence was observed for depth-to-width ratios $\zeta = L_x / L_z \leq 0.45$. The precise effect of the ζ as well as that of the bolt size on the analytic prediction (where a rigid link at the bolt position is assumed) is beyond the scope of this paper and will be published separately. The FE simulations in this paper are all conducted with a bolt size M20.

Fig. 2 shows a 2D sketch of a RC-EP connection, which is used for the derivation of analytical models as well.

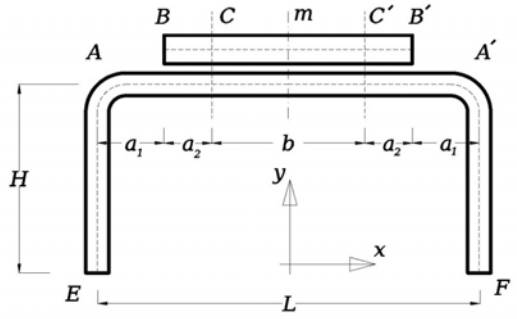

Fig. 2. Cross-section of the RC-EP system on a plane perpendicular to the column axis

2 ANALYTICAL APPROACH

2.1 Introduction

In the present section the RC – EP assembly will be modelled as a plane, two dimensional structure (*Fig.* 2). The purpose is to derive closed-form expressions predicting the initial stiffness characteristics of the connection with reasonable accuracy.

The interaction between RC/EP and its influence on the initial stiffness is affected by the effect of the contact status between the web of the RC and the EP. As the contact status varies radically with the direction of the applied normal force, the tension and the compression cases will be studied separately.

Closed-form expressions for the deflection of the RC/EP at specific points will be obtained by means of simple beam theory. These will be compared against FE results. It should be noted here that the effects of friction are not considered.

2.2 Reverse channel in tension

Actual contact zones are a priori unknown. However, if an assumption on the extend and the location of the contact length between the EP and the RC is made, the structural system of *Fig. 3* becomes trivial and its deflections can be derived from elementary beam-theory in terms of geometric and inertial characteristics of the parts that are involved. The effect of the bolt holes in the simplified beam-theory is neglected.

For the case of tension three different contact types depending on the bolt position ξ (*b/L*) could be identified:

1. *Contact type A: low values of ξ cause contact to appear between the bolts (CC)*
2. *Contact type B1: intermediate values of ξ lead to "mild" contact forces at the tail (BC)*
3. *Contact type B2: large values of ξ cause prying contact at the tip of the endplate (B)*

Particular values of ξ, for which contact patterns change, are related to the geometric characteristics of the RC-EP assemblies.

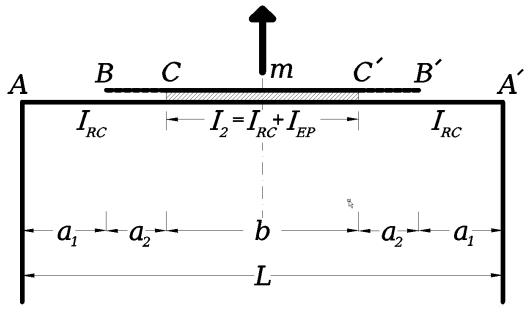

Fig. 3. Frame system for the case of contact between the bolts (type A)

For contact type A it is observed that the contact zone mainly develops in the vicinity of the bolts. This is due to the fact that a) the bolts constitute the only kinematic constraint between the RC and the EP along the length of segment *CC'* and b) the deformation induced to the endplate by the load at the middle. This assumption was verified by numerical simulations. This type of contact happens mostly when the endplate is thicker than the reverse channel and the bolt spacing relatively close.

The consequence is that the slope of the deflection line for both the RC and the EP beam elements can be assumed identical near the bolts. Therefore the moment of inertia I_2 of the frame analogon (*Fig.* 3) of the system along segment *CC'* may be taken as the sum of the moment of inertia of the endplate and reverse channel as shown in *Eq. (1)*. As slope locking is not perfect; a fact attributable to local deformation effects not being captured by simple beam theory, the moment of inertia of the EP is reduced.

$$I_2 = I_{\mathrm{RC}} + 0.6 I_{\mathrm{EP}} \left(1 - \xi\right) \tag{1}$$

Due to the particular form of the contact zone, the EP and RC beams develop equal rotations near the bolts and no frictional locking between the two is considered. Any additional contact between the EP and RC that might develop can only improve the validity of the assumption for I_2. The parts BC and B'C' of the endplate do not contribute to the stiffness of the system as they are not in contact with the reverse channel and behave as load-free cantilevers.

The rest of the 2D frame analogon is rather trivial. Using the method of transfer matrices [9], after some algebraic manipulations, the following expression is obtained:

$$u_{\mathrm{C}} = \frac{a^3 P}{6 E I_{\mathrm{RC}}} - \frac{\left(-a - \dfrac{2a^2 I_{\mathrm{C}}}{H I_{\mathrm{RC}}}\right)\left(abH I_{\mathrm{RC}} P + a^2 H I_2 P\right)}{-2EH I_{\mathrm{RC}} I_2 - 4bE I_{\mathrm{RC}} I_{\mathrm{C}} - 8aE I_2 I_{\mathrm{C}}} \tag{2}$$

Here $a = a_1 + a_2$ and I_{C} denotes the moment of inertia of the RC leg. The value u_{C} is the vertical displacement at the bolt due to a vertical force P, acting at the middle m of the endplate. The

stiffness of the reverse channel at the bolt is the inverse of the value of the displacement u_C for a value of $P = 0.5$.

Fig. 4 shows the structural systems for the derivation of contact type B1 and B2 with the following degrees of freedom:

$$u_{\mathrm{B1}}^{7} = \left[u_m^{\mathrm{RC}} \quad u_m^{\mathrm{EP}} \quad u_C \quad \varphi_C \quad u_B \quad \varphi_B \quad \varphi_A \right]^{\mathrm{T}} \tag{3}$$

$$u_{\mathrm{B2}}^{9} = \left[u_m^{\mathrm{RC}} \quad u_m^{\mathrm{EP}} \quad u_C \quad \varphi_C^{\mathrm{RC}} \quad u_B \quad \varphi_B^{\mathrm{RC}} \quad \varphi_A \quad \varphi_C^{\mathrm{EP}} \quad \varphi_B^{\mathrm{EP}} \right]^{\mathrm{T}} \tag{4}$$

In order to obtain a closed-formed solution for the simple structural systems described, the symbolic effective stiffness matrices are defined and solved considering the applied load. The meaning of the term "symbolic" is that every term of the stiffness matrix is derived using elementary beam theory. The task of the triangulation and back-substitution for a symbolic matrix is obtained by mathematical software. The detailed derivation and resulting expressions can be found in [8].

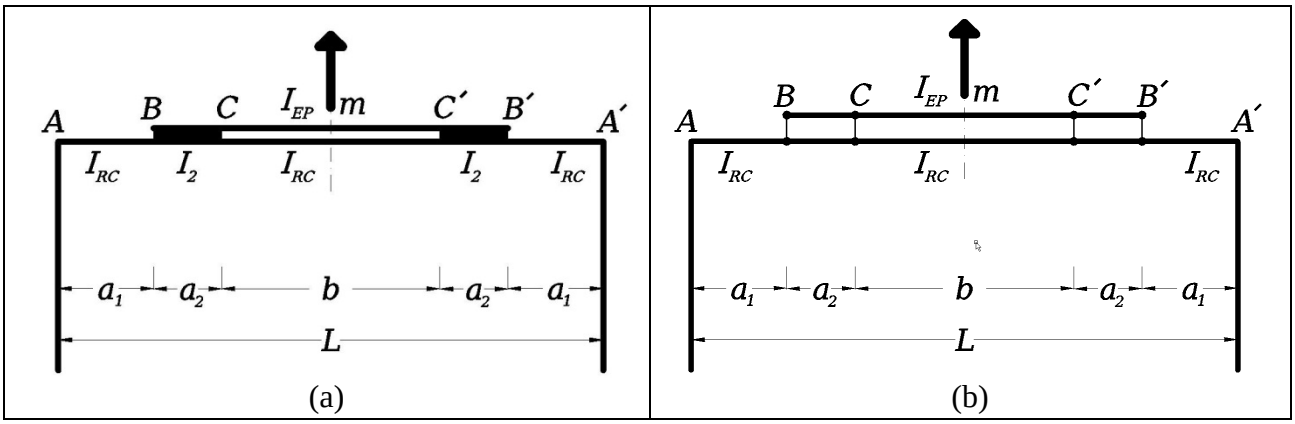

Fig. 4. Frame system for (a) "mild" contact forces (case B1) and (b) "prying" contact forces (case B2)

2.3 Reverse channel in compression

For the case of compression, the various stages of contact previously recognized for the tension cases, appear to happen in the reverse order. However, during the course of the numerical verification, it was realized that, for the case of compression, a single structural system may generate quite satisfactory results by way of introducing a certain correction factor. The structural system that produced the best results is that is that of *Fig. 3*. Using the transfer matrix method one gets the following expressions:

$$\begin{aligned}
A &= 2hI_{\mathrm{RC}}I_2(bI_{\mathrm{RC}}(12\,(a_1+a_2)^2 + 6\,b(a_1+a_2) + b^2) + 8I_2(a_1+a_2)^3) \\
B &= I_c(b^4I_{\mathrm{RC}}^2 + 8bI_{\mathrm{RC}}I_2(a_1+a_2)(4(a_1+a_2)^2 + 3b(a_1+a_2) + b^2) + 16(a_1+a_2)^4I_2^2) \\
C &= 48EI_{\mathrm{RC}}I_2(hI_{\mathrm{RC}}I_2 + 2I_c(bI_{\mathrm{RC}} + 2I_2(a_1+a_2))) \\
u_m^{\mathrm{compr}} &= \frac{(A+B)P}{4C}
\end{aligned} \tag{5}$$

where

$$I_2 = I_{\mathrm{RC}} + I_{\mathrm{EP}} \tag{6}$$

It was further found that the model complies much better with the plane-stress FE results if a shifting of the bolt position is introduced. Let the shifting length be:

$$S_b = \frac{a_2}{2}\sqrt{(1-\xi)} \tag{7}$$

The modified lengths b_s, a_{1s} are used in *Eq. (5)*.

$$\begin{aligned}
b_s &= b + 2S_b \\
a_{1s} &= a_1 - S_b
\end{aligned} \tag{8}$$

The shifting parameter was calibrated numerically. Through the use of it, it was possible to obtain a simpler (single formula) approximation for all types of contact.

2.4 Numerical verification

In this section 2D plane-stress FE models with unilateral contact are compared against frame theory derived analytic expressions, where the contact issue was dealt by assuming a contact zone between EP and RC. *Fig. 5 (a) and (b)* depict the very good agreement in both tension and compression. The vast majority falls within ± 5-10 %.

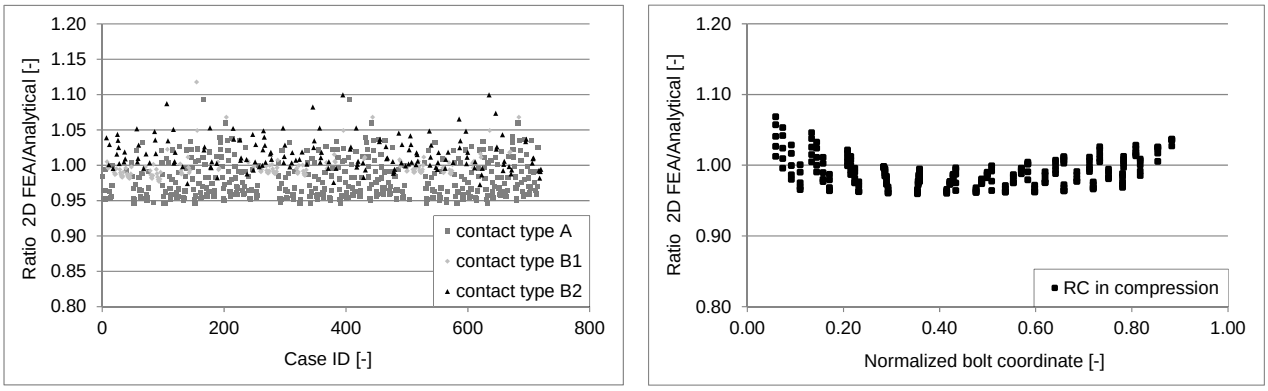

(a) (b)

Fig. 5. Comparison of analytical results vs. plane-stress FE results: (a) tension and (b) compression

Finally, the point of choosing the most appropriate analytic expression for the RC in tension without knowing the FEA result is addressed in *Fig.* 6. The axes are the normalized bolt coordinate $\xi = b/L$ and the ratio of the endplate thickness over that of the reverse channel t_{EP}/t_{RC}. It is clear that type-A and type-B contact arise within clearly defined, geometrically simple regions in the $(t_{EP}/t_{RC})\times(b/L)$ space. The type of expected contact for engineering applications should best be done by way of using *Fig. 6* as a nomograph.

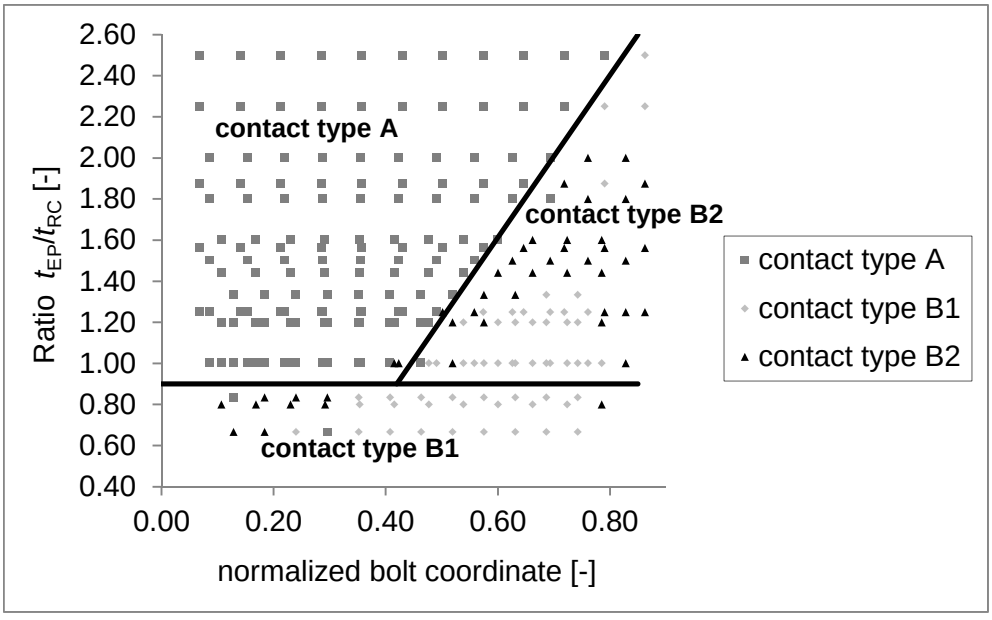

Fig. 6. Best approximating analytical expression – case of tension

3 CONCLUSIONS

This paper reports on analytical models derived for the initial stiffness prediction of reverse channel/partial-depth endplate connections at room and elevated temperatures.

The main conclusions are:

1. The technique of unilateral contact algorithms was found useful to derive the analytical expressions. Symbolic computation mathematical software enables to treat structural analysis problems in generalized way, thus leading to closed-form expressions.
2. Three different analytical models for the initial stiffness of reverse channel/partial-depth endplate connections subject to tension have been derived. They account for different types of contact interactions of the reverse channel and endplate, yielding to three formulae:
    a. Contact type A (contact between the bolts, 1 DOF system) as in *Eq. (2)*
    b. Contact type B1 (mild contact outside the bolts, 7 DOF system)
    c. Contact type B2 (prying contact outside the bolts, 9 DOF system)
3. For reverse channel/partial-depth endplate connections subject to compression *Eq. 5* is proposed for evaluating the stiffness.
4. All analytical models derived for predicting the initial stiffness of reverse channel/partial-depth endplate connections in compression and tension for width-to-depth ratios up to about 0.45 and a bolt M20 show accuracy of ± 10 %.

Although not presented in this paper, for width-to-depth ratios larger than 0.45 a linear correction factor may be introduced [8]. To cover the influence of the bolt stiffness, a quadratic regression analysis is currently undertaken to extend the analytical model.

ACKNOWLEDGEMENT

The research leading to these results has received funding from the European Community's Research Fund for Coal and Steel (RFCS) under grant agreement n° RFSR-CT-2009-00021. Furthermore, the first author gratefully acknowledges the additional funding provided by the European Regional Development Fund (NSS – Nordic Safety and Security).

REFERENCES

[1] European Committee for Standardization, 2005. EN 1993-1-8: Eurocode 3 - Design of steel structures, Part 1-8: Design of joints. Brussels.

[2] European Committee for Standardization, 2005. EN 1993-1-2: Eurocode 3 - Design of steel structures, Part 1-2: General rules - Structural fire design

[3] Gann RG, Grosshandler WL, Lew HS, Bukowski RW, Sadek F, Gayle FW, et al., 2008. Federal Building and Fire Safety Investigation of the World Trade Center Disaster: Structural Fire Response and Probable Collapse Sequence of World Trade Center Building 7. Washington.

[4] Federal Emergency Management Authority F, 2002. World Trade Center Building Performance Study. Washington.

[5] Newman GM, Robinson JT, Bailey CG, 2006. Fire safe design: a new approch to multi-storey steel-framed buildings. 2nd ed. Ascot. Steel Construction Institute

[6] Hicks SJ, Newman GM, Edwards M, Orton A, 2002. Design Guide for Concrete Filled Columns. London. Corus Tubes/The Steel Construction Institute

[7] Lopes F, Santiago A, Simões da Silva L, Heistermann T, Veljkovic M, Guilherme da Silva J, 2013. Experimental Behaviour of the Reverse Channel Joint Component at Elevated and Ambient Temperatures. Int J Steel Struct 2013;13:459–72

[8] Heistermann T, 2013. Stiffness of Reverse Channel Connections at Room and Elevated Temperatures. Doctoral Thesis. Luleå University of Technology

[9] Pilkey WD, 2005. Formulas for stress, strain and structural matrices. John Wiley & Sons Ltd.